Dalton Transactions

Accepted Manuscript

This article can be cited before page numbers have been issued, to do this please use: S. Muniyandi, P. Vadivelu and M. Palaniandavar, *Dalton Trans.*, 2017, DOI: 10.1039/C7DT00576H.

ROYAL SOCIETY OF CHEMISTRY

rsc.li/dalton

View Article Online
DOI: 10.1039/C7DT00576H

Manuscript Type: DT-ART-02-2017-000576-R1
Manuscript submitted to: ***Dalton Trans.***

Novel nickel(II) complexes of sterically modified linear N4 ligands: Effect of donor atom type, steric hindrance, diamine backbone and solvent on nickel(II) spin state and alkane hydroxylation with *m*-CPBA as oxidant

Muniyandi Sankaralingam,[a] Prabha Vadivelu,[b] and Mallayan Palaniandavar[a]*

[a]*School of Chemistry, Bharathidasan University, Tiruchirappalli - 620024, Tamil Nadu, India*

[b]*Chemical Sciences and Technology Division, National Institute for Interdisciplinary Science and Technology, CSIR, Trivandrum-695019.*

*To whom correspondence should be addressed, e-mail: palanim51@yahoo.com and palaniandavarm@gmail.com, Fax : +91-431-2407045

View Article Online
DOI: 10.1039/C7DT00576H

Abstract

A series of Ni(II) complexes of the types $[Ni(L)(CH_3CN)_2](BPh_4)_2$ **1**-**3**, **5** and $[Ni(L4)](BPh_4)_2$ **4**, where L = *N*,*N'*-bis(2-pyrid-2-ylmethyl)-1,4-diazepane (L1), *N*-(6-methylpyrid-2-ylmethyl)-*N'*-(pyrid-2-ylmethyl)-1,4-diazepane (L2), and *N*,*N'*-bis(6-methyl-2-pyridylmethyl)-1,4-diazepane (L3), *N,N*'-dimethyl-*N,N'*-bis(2-pyridylmethyl)ethylenediamine (L5) and L4 = *N*,*N'*-bis(1-methyl-1H-imidazole-2-yl)methyl)-1,4-diazepane, has been isolated and characterized. The complex cations of **1** and **4** possess respectively distorted octahedral and low-spin square planar coordination geometries in which nickel(II) is meridionally coordinated to all the four nitrogen atoms of L1 and L4. DFT studies reveal that L5 with ethylenediamine back bone coordinates in *cis*-β mode in $[Ni(L5)(CH_3CN)_2]^{2+}$ **5**, but in *cis*-α mode in $[Ni(L5)(H_2O)_2]^{2+}$. Also, it illustrates the role of ligand donor atom type, diazacyclo back bone and steric hindrance to coordination of pyridyl nitrogen in conferring novel coordination geometries on Ni(II). All the complexes catalyze the oxidation of cyclohexane in the presence of *m*-CPBA as oxidant up to 600 turnover numbers (TON) with relatively good alcohol selectivity (A/K, 5.6-7.2). Adamantane is oxidized to 1-adamantanol, 2-adamantanol and 2-adamantanone with high bond selectivity (3°/2°, 8.7-11.7). The incorporation of methyl substituent(s) on one (**2**) or both (**3**) the pyridyl rings as well as and the replacement of both the pyridylmethyl arms in **1** by imidazolylmethyl arms to give **4** decrease the catalytic efficiency. Interestingly, **5** with *cis*-β mode of coordination provides two labile *cis* coordination sites for oxidant binding, leading to higher total TON and product/bond selectivity.

View Article Online
DOI: 10.1039/C7DT00576H

Introduction

Nature utilizes a variety of copper[1] and iron[2-4] containing enzymes to catalyze a variety of biologically essential transformations. Among the iron enzymes cytochrome P450, bleomycin and methane monooxygenases, soluble methane monooxygenases (sMMO) are the widely investigated metalloenzymes that catalyze the oxidation of methane to methanol using molecular oxygen under ambient conditions.[2-4] Inspired by the sMMO enzyme activity, several low molecular weight diiron(II)/(III) complexes have been isolated and investigated as catalysts for alkane hydroxylation, epoxidation and sulfoxidation reactions.[5-7] Also, such a study can lead to a better understanding of the spectral and structural properties of the active sites and shed light on the catalytic activity of the enzymes. Currently, the study of catalytic oxidation of saturated hydrocarbons under mild conditions has received greater attention and has become an exciting and challenging scientific goal, because conventional hydroxylation processes usually require high pressure and high temperature.[8] Though iron complexes are considered as the potential catalysts for this industrially important reaction, a variety of low molecular weight compounds of transition metals like Mn, Co, Ni, Cu, Ru and Os has been isolated and investigated as alkane oxidation catalysts.[9-13,14-35]

In very recent times, nickel complexes have attracted much attention as catalysts for alkane hydroxylation. Several dinuclear nickel(II) oxo-bridged,[14-15,21,17] and mononuclear nickel(III)-peroxo[16a,16c,22] and nickel(II)-superoxo[16b,18,19,23,24] complexes have been reported as reactive intermediates in the oxidation. Itoh *et. al*. have demonstrated[25] that [Ni(TPA)(OAc)(H_2O)](BPh_4), where TPA is tris(pyrid-2-yl-methyl)amine, is a very efficient and robust turnover catalyst for alkane hydroxylation with *m*-chloroperbenzoic acid (*m*-CPBA) as oxidant. Later they isolated a series of Ni(II) complexes of linear N3,[26] tripodal N4[25,26] and tripodal mono- (N3O)[26], bis- and tris(phenolate)[27a] ligands and studied them as catalysts for oxidation of cyclohexane using *m*-CPBA. Very Recently, they have shown that Ni(II) complexes of tetradentate N4 ligands catalyze the direct hydroxylation of benzene to phenol using hydrogen peroxide.[27b] Recently, Hikichi *et. al*. have isolated a nickel(II)-alkylperoxo complex to study its catalytic activity towards oxidation of alkanes,[28] and later studied the ability of nickel(II)-acylperoxo complexes to effect oxygenation of olefins, sulfides and alkane with *m*-CPBA.[29] We have isolated a few nickel(II) complexes of tripodal N4,[30] and pentadentate N5[31] ligands and a number of mixed ligand[32] nickel(II) complexes as catalysts for alkane hydroxylation using *m*-

View Article Online
DOI: 10.1039/C7DT00576H

CPBA as oxidant. We observed an interesting linear correlation between the metal-ligand covalency parameter (β) and the total turnover number (TON),[30] and illustrated the importance of ligand denticity, Lewis acidity of Ni(II) center and π-back bonding in determining the catalytic activity.[32] We established a high-spin (S = 3/2) $[(N5)Ni^{II}\text{-}O^{\bullet}]^{+}$ species as the ground state in cyclohexane hydroxylation reactions, and predicted an overall two spin-state reactivity with H-abstraction as the rate-determining step.[31] Kallol Ray *et.al*. trapped and characterized the Ni^{III}=O/ Ni^{III}-OH intermediate species in the reaction of a nickel(II) salt with *m*-CPBA.[33] Very recently, a Ni^{III}-oxyl intermediate has been shown to perform hydrogen atom abstraction (HAA) of weak C-H bonds and oxygen atom transfer (OAT) to thioanisoles and styrene.[34] Also, McDonald *et. al*. have reported[35] a terminal nickel(III)–oxygen adduct that performs hydrogen atom abstraction and oxygen atom transfer. A few mono- and dinuclear Ni(II) complexes have been reported now as catalysts for olefin epoxidation.[36]

Thus, nickel(II) complexes have the potential to be developed as efficient alkane hydroxylation catalysts. So, we continue to isolate nickel(II) complexes, study the effect of ligand stereoelectronic factors upon the catalytic efficiency and alcohol selectivity in alkane hydroxylation. Herein we report a few novel nickel(II) complexes of systematically varied tetradentate N4 ligands containing cyclic diamine backbone and different heterocyclic nitrogen atoms as pendants (Scheme 1). Such N4 ligands are expected[30] to make available at least two labile coordination sites for binding with the oxidant *m*-CPBA, leading to high catalytic activity. We aim to investigate the effect of incorporating pyridyl, sterically hindered 6-methylpyridyl, and strongly σ-bonding imidazolyl nitrogen in dictating the nickel(II) coordination geometry and hence the catalytic activity and alcohol/bond selectivity. Also, we have isolated a Ni(II) complex of the ethylenediamine based ligand L5 to examine the effect of incorporating diazacycloalkane ligand back bone upon coordination geometry and hence reactivity. Density functional theory calculations illustrate the ability of bis(imidazolyl) ligand L4 and other related ligands to confer a low-spin configuration on Ni(II), and also the effect of coordinated solvent on the mode of coordination of L5. The present ligand systems with diazapane backbone coordinate meridionally to Ni(II) and tend to form square pyramidal coordination geometry with the axial site available for binding of oxidant. We have found that all the complexes catalyze the hydroxylation of cyclohexane and adamantane efficiently within six hours with good alcohol to ketone selectivity (A/K, 5.6-7.2) in the presence of *m*-CPBA as oxidant.

View Article Online
DOI: 10.1039/C7DT00576H

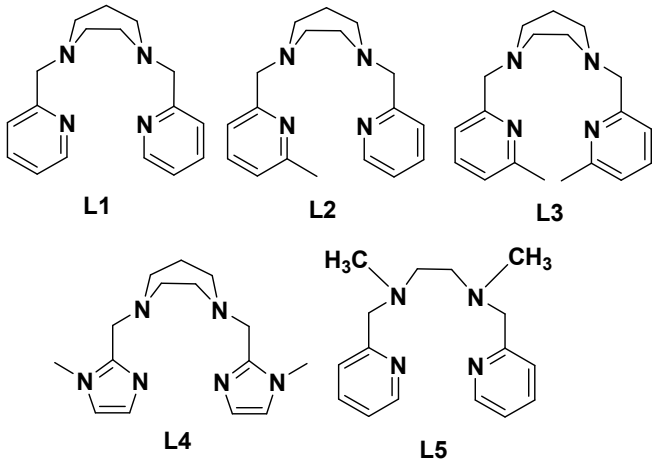

Scheme 1. Molecular structures of tetradentate N4 ligands employed in the study

Experimental

Materials

Pyridine-2-carboxaldehyde, *N,N'*-dimethylethylenediamine, homopiperazine, nickel(II) perchlorate hexahydrate, adamantane, *m*-chloroperbenzoic acid, sodium tetraphenylborate, 1-methylimidazole-2-carboxaldehyde (Aldrich), 6-methylpyridine-2-carboxldehyde, sodium triacetoxyborohydride (Alfa Aesar), acetic acid glacial, ethyl acetate, triethylamine, sodium sulphate (Merck, India), cyclohexane (Ranbaxy) were used as received. Dichloromethane, diethylether, tetrahydrofuran, acetonitrile (Merck, India) and methanol (Sisco Research Laboratory, Mumbai) were distilled before use.

Synthesis of ligands

The ligands *N,N'*-bis(2-pyrid-2-ylmethyl)-1,4-diazepane (L1), *N*-(6-methylpyrid-2-ylmethyl)-*N'*-(pyrid-2-ylmethyl)-1,4-diazepane (L2), and *N,N'*-bis(6-methyl-2-pyridylmethyl)-1,4-diazepane (L3), *N,N'*-bis(1-methyl-1H-imidazole-2-yl)methyl)-1,4-diazepane (L4) and *N,N*'-dimethyl-*N,N'*-bis(2-pyridylmethyl)ethylenediamine (L5) were prepared using the previously reported procedures.[37,38]

Isolation of Ni(II) complexes

$[Ni(L1)(CH_3CN)_2](BPh_4)_2$ (1). A methanol solution (5 mL) of $Ni(ClO_4)_2 \cdot 6H_2O$ (0.365 g, 1 mmol) was added to a methanol solution (5 mL) of L1 (0.282 g, 1 mmol) with stirring at room temperature. The color of the solution turned to indigo. The solution was stirred for additional 30 min and the color of solution turned to blue. Then followed by the metathesis of the above

View Article Online
DOI: 10.1039/C7DT00576H

complex by adding $NaBPh_4$ (0.684 g, 2 mmol) in acetonitrile. The pink colored precipitate was filtrated off, washed with small quantities of ice-cold methanol and then dried. Single crystals suitable for X-ray crystallographic analysis were obtained by slow evaporation of CH_3CN/CH_2Cl_2 solution of the complex. Yield, 0.89 g, 84%. Anal. Calcd. for $C_{69}H_{68}N_6B_2Ni$: C, 78.06; H, 6.46; N, 7.92. Found: C, 78.36; H, 6.42; N, 7.83. ESI-MS: *m*/*z* 170.20 $[(M-2CH_3CN-2BPh_4)^{2+}]$.

The complexes **2-4** were prepared by using the procedure employed for isolating **1** and using the ligands **L2**–**L4**.

$[Ni(L2)(CH_3CN)_2](BPh_4)_2$ (2). Pink color, Yield, 0.849 g, 79%. Anal. Calcd. for $C_{70}H_{70}N_6B_2Ni$: C, 78.16; H, 6.56; N, 7.81. Found: C, 78.36; H, 6.43; N, 7.73. ESI-MS: *m*/*z* 177.12 $[(M-2CH_3CN-2BPh_4)^{2+}]$.

$[Ni(L3)(CH_3CN)_2](BPh_4)_2$ (3). Pink color, Yield 0.81 g, 75%. Anal. Calcd. for $C_{71}H_{72}N_6B_2Ni$: C, 78.26; H, 6.66; N, 7.71. Found: C, 78.14; H, 6.59; N, 7.76. ESI-MS: *m*/*z* 184.14 $[(M-2CH_3CN-2BPh_4)^{2+}]$.

$[Ni(L4)](BPh_4)_2$ (4). Yellow color, Yield 0.89 g, 91%. Anal. Calcd. for $C_{63}H_{64}N_6B_2Ni$: C, 76.78; H, 6.55; N, 8.53. Found: C, 76.81; H, 6.58; N, 8.45. ESI-MS: *m*/*z* 173.11 $[(M-2BPh_4)^{2+}]$. Single crystals suitable for X-ray crystallographic analysis were obtained by slow evaporation of CH_3CN/CH_2Cl_2 solution of the complex.

$[Ni(L5)(CH_3CN)_2](BPh_4)_2$ (5). Pink color, Yield 0.74 g, 71%. Anal. Calcd. for $C_{68}H_{68}N_6B_2Ni$: C, 77.81; H, 6.53; N, 8.01. Found: C, 77.88; H, 6.48; N, 8.10. ESI-MS: *m*/*z* 164.14 $[(M-2CH_3CN-2BPh_4)^{2+}]$.

Caution*! Perchlorate salts of the compounds are potentially explosive. Only small quantities of these compounds should be prepared and suitable precautions should be taken when they are handled*.

Physical measurements

Elemental analyses were performed on a Perkin Elmer Series II CHNS/O Analyzer 2400. ^1H NMR spectra were recorded on a Bruker 400 MHz NMR spectrometer. All the ligands were purified on TELEDYNE CombiFlash Rf Flash chromatography. Electronic spectra were recorded on an Agilent 8453 Diode Array Spectrophotometer. ESI-MS analyses were recorded on a Micromass Quattro II triple quadrupole mass spectrometer. The products were analyzed by

View Article Online
DOI: 10.1039/C7DT00576H

using Hewlett Packard (HP) 6890 GC series Gas Chromatograph equipped with a FID detector and a HP-5 capillary column (30 m × 0.32 mm × 2.5 μm). GC-MS analysis was performed on an Agilent GC-MS equipped with 7890A GC series (HP-5 capillary column) and 5975C inert MSD under conditions that are identical to that used for GC analysis.

Computational details

The geometry optimization of complexes have been performed with the B3LYP method using Gaussian 09 program.[39] The metal center was described with the Stuttgart RECPs and associated basis sets (SDDALL)[40] and all other atoms with the 6-31G** basis sets.[41]

Crystallographic data collection, refinement and structure solution

The diffraction experiments were carried out for **1** an OXFORD XCALIBUR diffractometer and for **4** data was collected using Bruker SMART APEX diffractometer both equipped with a CCD area. The single crystals of **1** were mounted on a glass fiber in paraffin oil and then brought into the cold nitrogen stream of a low temperature device so that the oil solidified. Intensity data for the crystals were collected using MoKα (λ = 0.71073 Å) radiation on OXFORD XCALIBUR diffractometer equipped with a CCD area detector at low temperature. Empirical absorption correction using spherical harmonics, implemented in SCALE3 ABSPACK scaling algorithm was applied.[42] The structure was solved by direct methods using the SHELXS and refined on F^2 by the full-matrix least-squares technique SHELXL-2016/6.[43] The single crystals of **4** data were collected at room temperature. An empirical absorption correction was applied to the collected reflections with SADABS.[44] The structure was solved by heavy atom method and other non-hydrogen atoms were located in successive difference Fourier syntheses. Final cycles of least-squares refinements with the modified data set improved both the R-values and Goodness of Fit significantly. Hydrogen atoms attached to the ligand moiety were located from the difference Fourier map. Crystal data and additional details of the data collection and refinement of the structure are presented in Table 1. The selected bond lengths and bond angles are listed in Table 2.

View Article Online
DOI: 10.1039/C7DT00576H

Catalytic oxidations

The oxidation of alkanes was carried out under nitrogen atmosphere at room temperature within six hours. In a typical reaction, nickel(II) complex (0.35×10^{-6} mol dm^{-3}) was added to a mixture of alkanes (2.45 mol dm^{-3}) and oxidant *m*-CPBA (0.35 mol dm^{-3}) in CH_2Cl_2:CH_3CN mixture (3:1 v/v). After 6 hr the reaction mixture was quenched with triphenylphosphine and filtered over a silica column and then eluted with diethylether. An internal standard (bromobenzene) was added at this point and the solution was subjected to GC analysis. The mixture of organic products was identified by Agilent GC-MS and quantitatively analyzed by HP 6890 series GC equipped with HP-5 capillary column (30 m × 0.32 mm × 2.5 μm) using a calibration curve obtained with authentic compounds. All of the products were quantified using GC (FID) with the following temperature program: injector temperature 130 °C; initial temperature 60 °C, heating rate 10 °C min^{-1} to 130 °C, increasing the temperature to 160 °C at a rate of 2 °C min^{-1}, and then increasing the temperature to 260 °C at a rate of 5 °C min^{-1}; FID temperature 280 °C. GC-MS analysis was performed under conditions identical to those used for GC analysis. The averages of three measurements are reported.

Results and discussion

Synthesis and characterization of ligands and complexes

The ligands L1, L3 and L4 were prepared according to a known reductive amination procedure[37] by treating one equivalent of homopiperazine with two equivalents of the corresponding aldehydes and using sodium triacetoxyborohydride as reducing agent. The ligand L2 (Scheme 1) was synthesized by a two step procedure involving selective substitution of 2-(chloromethyl)pyridine with homopiperazine in the presence of triethylamine, followed by reductive amination with 6-methylpyridine-2-carboxaldehyde.[10b] The ligand L5 was synthesized by substitution reaction with *N,N'*-dimethylethylenediamine and picolylchloride hydrochloride by using the previously reported procedure.[38] All the ligands were characterized by ^{1}H NMR. The nickel(II) complexes **1**–**5** were prepared by adding one equivalent of ligand to a methanol solution of $Ni(ClO_4)_2 \cdot 6H_2O$, followed by the addition of sodium tetraphenylborate in acetonitrile solvent. They are formulated as $[Ni(L)(CH_3CN)_2](BPh_4)_2$ **1**-**3**, **5** and $[Ni(L4)](BPh_4)_2$ **4** on the basis of elemental analysis, UV-Visible spectroscopy, mass spectrometry and the X-ray crystal structures of **1** and **4** confirm it. The pyridyl and sterically hindering 6-methylpyridyl and

View Article Online
DOI: 10.1039/C7DT00576H

imidazolyl moieties are expected to determine the structural and electronic properties and catalytic activities of the complexes towards alkane hydroxylation. Thus, interestingly, nickel(II) complexes **1**–**4** of ligands with diaza cyclic diamine backbone possess *trans* coordination geometry (Scheme 2), whereas **5** with ethylenediamine backbone possesses *cis*-α or *cis*-β configuration depending on solvent of coordination.

Description of structures of $[Ni(L1)(CH_3CN)_2](BPh_4)_2$ 1 and $[Ni(L4)](BPh_4)_2$ 4

The molecular structures of complex cations of $[Ni(L1)(CH_3CN)_2](BPh_4)_2$ **1** and $[Ni(L4)](BPh_4)_2$ **4** are shown in Fig. 1 and Fig. 2 respectively, together with atom numbering scheme and the principal bond lengths and bond angles are collected in Table 2, respectively. The complex cation of **1** possesses a NiN_6 coordination sphere with a distorted octahedral coordination geometry constituted by two pyridyl and two tertiary amine nitrogen atoms of the linear tetradentate ligand and two acetonitrile molecules. The ligand L1 is meridionally coordinated conferring a *trans* coordination geometry on Ni(II). The Ni-N_{py} (2.065, 2.076 Å) and Ni-N_{amine} (2.075, 2.077 Å) bond distances fall in the ranges observed for the previously reported nickel(II) complexes (Ni-N_{py}, 2.0451 – 2.1692, Ni-N_{amine}, 1.926 - 2.196 Å),[25-27,30-32] and are close to those observed (Ni-N_{py}, 2.057 - 2.060, Ni-N_{amine}, 2.052 – 2.054 Å) for $[Ni(L1)Cl]^+$ already reported.[45] The Ni-$N2_{py}$ bond length (2.065(2) Å) is shorter than the Ni-N_{amine} bond lengths (2.075(2), 2.077(2) Å) due to sp^2 and sp^3 hybridization of pyridyl and amine nitrogen donors respectively. However, the Ni-$N2_{py}$ bond (2.065(2) Å) is slightly shorter than the Ni-$N6_{py}$ bond (2.076(3) Å). The nitrogen atoms of both the acetonitrile molecules are coordinated less strongly than the other four nitrogen atoms of L1, as expected. Further, the Ni-$N8_{ACN}$ bond (2.184(3) Å) is longer than the Ni-$N10_{ACN}$ bond (2.097(3) Å) as it is oriented along the sterically hindering trimethylene side of diazapane ring. The N-Ni-N (77.63(10)° - 117.22(10)°) and N-Ni-N (159.69(10)° - 164.92(10)°) bond angles deviate from the ideal octahedral angles of 90° and 180° respectively, revealing that the octahedral coordination geometry around Ni(II) is significantly distorted.

The meridional coordination of L1 resulting in *trans* coordination geometry in **1** is similar to that found in $[Mn(L1)Cl_2]$[10c] with a distorted octahedral coordination geometry, and $[Mn(L1)(CH_3CN)_3]^{2+}$ [46] with a seven-coordinate distorted pentagonal bipyramidal geometry. Also, the ligand L1 has been predicted[6a] to coordinate meridionally to iron(II) in the *in situ*

View Article Online
DOI: 10.1039/C7DT00576H

generated complex species $[Fe(L1)(CH_3CN)_2]^{2+}$. The ligand 1,5-bis(2-pyridylmethyl)-1,5-diaza-cyclooctane, analogous to L1, has been shown to form square planar as well as square pyramidal Ni(II) complexes.[47] Interestingly, this is in contrast to the folded geometry of linear N4 ligands with ethylenediamine backbone, which confer *cis*-α or *cis*-β octahedral coordination geometries on Ni(II) (Scheme 2). Thus, the linear ligand L5, which is the ethylenediamine analogue of L1, forms the high-spin complexes $[Ni(L5)Cl_2]\cdot H_2O$[48a], $[Ni(L5)(H_2O)_2]^{2+}$ [48b] and $[Ni(L5)(OAc)(H_2O)]^{+}$ [48b], all of which possess octahedral coordination geometry with *cis*-α

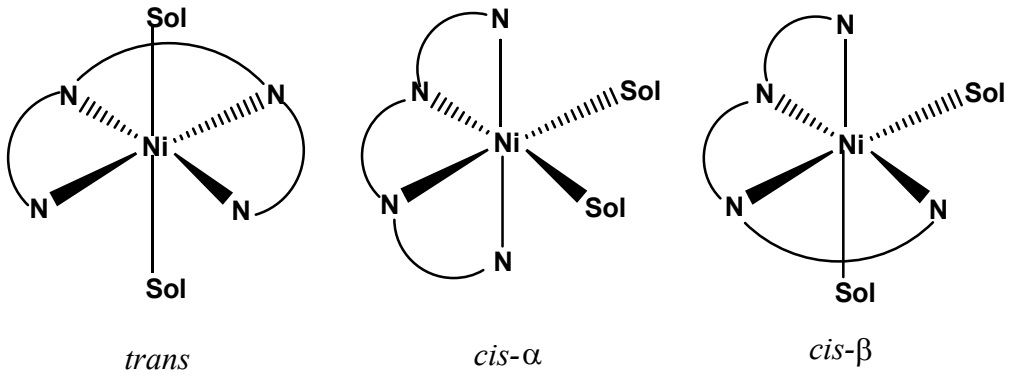

Scheme 2. Different octahedral configurations adopted by tetradentate N4 ligands

configuration. The *cis*-α coordination of L5 is similar to that found in $[Fe(L5)(CH_3CN)_2]^{2+}$ [5c] and $[Mn(L5)Cl_2]$.[49] On the other hand, interestingly, in the iron(III) tetrachlorocatecholate adduct $[Fe(L1)(cat)]^{+}$, sterically encumbered ligand L1 is bound with a *cis*-β configuration,[37] revealing that the mode of coordination of N4 ligands with diazapane backbone depends on the metal ion and the secondary ligand.

The molecular structure of $[Ni(L4)](BPh_4)_2$ **4** consists of a discrete $[Ni(L4)]^{2+}$ cation and two BPh_4^- counter anions (Fig. 2). The NiN_4 coordination sphere of the complex cation shows a distorted square planar coordination geometry constituted by two imidazole and two tertiary amine nitrogen atoms of meridionally coordinated ligand L4 with its diazacyclo ligand back bone in normal boat conformation. The observed Ni-N bond lengths (1.869-1.915 Å) and bond angles are in agreement with those observed for the previously reported square planar Ni(II) complexes.[45,50] The Ni-N_{im} bonds (1.869(3), 1.892(3) Å) are shorter than the Ni-N_{amine} bonds (1.909(3), 1.915(3) Å) on account of sp^2 and sp^3 hybridization of imidazole and amine nitrogens respectively. The N-Ni-N (82.83(14)° - 103.25(16)°) and N-Ni-N (167.46(15)° - 170.72(14)°)

View Article Online
DOI: 10.1039/C7DT00576H

bond angles deviate from the ideal square planar angles of 90° and 180° respectively, revealing that there is significant distortion in the square planar coordination geometry. Similar low-spin square planar coordination geometry has been observed for Ni(II) complexes of meridionally coordinating tetradentate N4 ligands 1,4-bis(imidazol-4-ylmethyl)-1,4-diazepane,[45] and 1,4-bis(3-methylimidazol-4-ylmethyl)-1,4-diazacycloheptane.[50] Also, the ligand L1, which forms the octahedral complex $[Ni(L1)(CH_3CN)_2](BPh_4)_2$ **1** (cf. above), also forms the low-spin square planar complex $[Ni(L1)]^{2+}$ as well as high-spin square pyramidal complex$[Ni(L1)Cl]^{+}$ (Scheme 3).[45] As imidazole is a base stronger than pyridine [pK_a (BH^+): pyridine, 5.2; imidazole, 7.01], both the Ni-N_{im} bonds (1.869 - 1.892 Å) in **4** are shorter than the Ni-N_{py} bonds (1.906 - 1.927 Å)

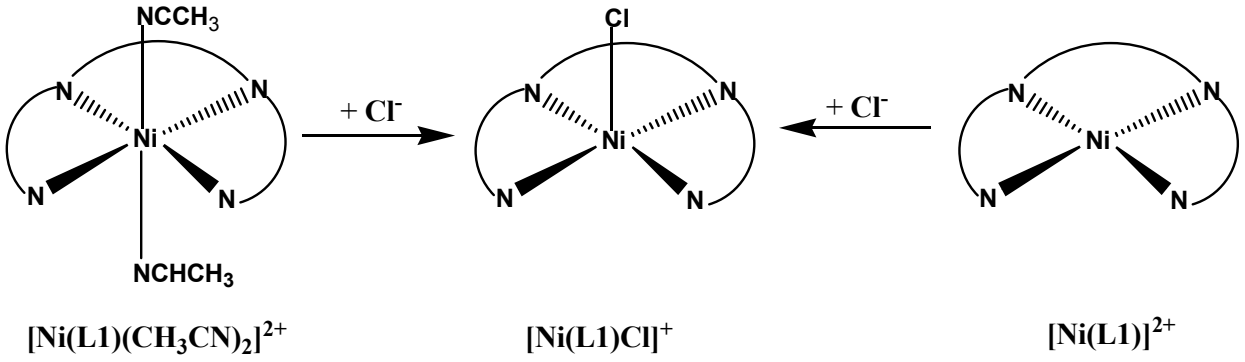

Scheme 3. Different coordination geometries adopted by L1 ligand: $[Ni(L1)(CH_3CN)_2](BPh_4)_2$ **1** (this work), $[Ni(L1)Cl]^{+}$ [45], and $[Ni(L1)]^{2+}$ [45]

in $[Ni(L1)]^{2+}$.[45] Further, the L1 and L4 ligands support a square pyramidal coordination geometry for $[Ni(L1)Cl]^{+}$ [45] and $[Ni(L4)Cl]^{+}$ [45] (τ, 0.028), both with a high-spin configuration; the Ni-N_{im} (2.000, 2.010 Å) and Ni-N_{amine} (2.091, 2.112 Å) bonds are longer than those observed here for low-spin $[Ni(L4)]^{2+}$ complex, as expected (cf. above). Thus, the present N4 ligand systems with diazapane backbone display the ability to confer a range of coordination geometries (**Scheme 3**).

DFT studies: Structures of nickel(II) complexes

DFT studies have been carried out to understand the effect of incorporating methyl substituent(s) on pyridyl ring(s) and replacing pyridyl nitrogen by imidazolyl nitrogen on the ability of ligands to form complexes with low-spin configuration. The optimized geometries of **1** and **4** agree well with those in their X-ray crystal structures (cf. above), suggesting that the

View Article Online
DOI: 10.1039/C7DT00576H

optimized structures of **1**-**5** are reliable in understanding the structural variations (Fig. 3, Fig. 4 and Fig. S1 see in supporting information, ESI †). Upon incorporating a methyl substituent in **1** to obtain **2**, the terminal Ni-N_{py} bonds are elongated (**1**: Ni-$N1_{py}$, 2.12; Ni-$N4_{py}$, 2.12; **2**: Ni-$N1_{py}$, 2.22; Ni-$N4_{py}$, 2.21 Å) with the Ni-N_{amine} bonds remaining almost unaffected, and concomitantly, the Ni-N_{ACN} bonds are shortened (**1**: 2.26, 2.17; **2**: 2.21, 2.14 Å). Similarly, upon incorporating a methyl substituent on the other pyridine ring in **2** to get **3**, the terminal Ni-$N4_{py}$ bond is elongated further though the Ni-$N1_{py}$ bond is slightly shortened (Ni-$N1_{py}$, 2.20; Ni-$N4_{py}$, 2.27 Å) with the Ni-N_{amine} bonds affected only slightly. Interestingly, the Ni-$N5_{ACN}$ bond is shortened further (2.19 Å) and the Ni-$N6_{ACN}$ bond is elongated slightly (2.17 Å). Thus, the effect of incorporating sterically hindering methyl substituent(s) on the terminal pyridyl ring(s) in **1** to obtain **2** and **3** is to shorten the trans axial bonds formed by solvent molecules, which has a very important consequence on the reactivity of complexes (cf. below). The optimized structure of $[Ni(L5)(CH_3CN)_2]^{2+}$ **5** exhibits a distorted octahedral *cis*-β coordination geometry; however, $[Ni(L5)(H_2O)_2]^{2+}$ **5a** (Fig. S2 in ESI †) exhibits a distorted octahedral *cis*-α coordination geometry, which is found in the X-ray crystal structure of $[Ni(L5)(H_2O)_2]^{2+}$.[48] This interesting observation illustrates that the nature of coordinated solvent determines the mode of coordination of ethylenediamine-based linear N4 ligands. The calculated bond distances for **5** (Ni-N_{py}, 2.11, 2.14; Ni-N_{amine}, 2.17,2.20 Å) and **5a** (Ni-N_{py}, 2.16, 2.21; Ni-N_{amine}, 2.18, 2.21 Å) are in reasonably good agreement with those (Ni-N_{py}, 2.074, 2.104; Ni-N_{amine}, 2.160 Å) determined experimentally for $[Ni(L5)(H_2O)_2]^{2+}$.[48] Interestingly, the optimized structures of both $[Ni(pdao)(H_2O)_2]^{2+}$ **6** and $[Ni(pdao)(CH_3CN)_2]^{2+}$ **6a** (pdao = 1,8-bis(2-pyridyl)-3,6-dimethyl-3,6-diazaoctane) possess an octahedral *cis*-α coordination geometry (Fig. S1, S2 in ESI †), which is in good agreement with the experimentally observed one for **6**.[48a] This is expected as the 5,6,6,5 chelate ring system formed by pdao is more flexible than the 5,5,5,5 chelate ring system in **5** and **5a**.

To understand the ability of L4 ligand with diazapane back bone to confer a low-spin square planar configuration on Ni(II), the optimized electronic structures of **1**-**6** with high- (S = 1) and low-spin (S = 0) configurations have been computed (Fig. 3, Fig. S1 in ESI†).[39] The complexes **1**-**3**, **5** and **6** possess high-spin ground states which are more stable than the corresponding low-spin states by +11.0, +26.1, +19.4, +28.0 and +22.0 kcal/mol respectively. In the high-spin state, all the complexes, as expected, show an octahedral coordination geometry in

View Article Online
DOI: 10.1039/C7DT00576H

which acetonitrile molecules are coordinated in trans positions and the two unpaired electrons are found mostly on the Ni(II) center while the low-spin complexes exhibit distorted four-coordinate geometries. The optimized low-spin structure ($\mathbf{4}_{ls}$) exhibits a square planar geometry, as seen in the X-ray crystal structure of **4**, whereas the optimized high-spin structure ($\mathbf{4}_{hs}$) shows a distorted square planar coordination geometry with all the four Ni-N bonds being weaker than those in $\mathbf{4}_{ls}$. It is clear that two solvent molecules are required to coordinate to Ni(II) to form a stable distorted octahedral geometry as for $\mathbf{1}_{hs}$. And, notably, the $\mathbf{4}_{ls}$ structure is computed to be more stable than $\mathbf{4}_{hs}$ by +5.8 kcal/mol only. The computed structures of **1-5** are useful in illustrating their potential as catalysts for alkane oxidation (cf. below).

Electronic spectral properties

The electronic spectral data of all the Ni(II) complexes are summarized in Table 3 and the typical electronic absorption spectrum of **1-5** is shown in Fig. 5. In CH_2Cl_2:CH_3CN (3:1 v/v) solvent mixture, all the complexes, except **4**, exhibit two well-defined absorption bands (470–565, 840–924 nm) together with an absorption spectral feature on the low energy band. The lower energy band is assigned to $^3A_{2g} \rightarrow {}^3T_{2g}(F)$ (ν_1) transition and the higher energy band to $^3A_{2g} \rightarrow {}^3T_{1g}(F)$ (ν_2) transition while the feature located on the low energy band is assigned to $^3A_{2g} \rightarrow {}^1E_{1g}(D)$ spin-forbidden transition in Ni(II) located in an octahedral environment.[30-32,51] The intense shoulder observed in the range 355–385 nm is assigned to $^3A_{2g} \rightarrow {}^3T_{1g}(P)$ (ν_3) transition. All these assignments are in good agreement with those observed for the previously reported octahedral Ni(II) complexes.[30-32,48a,51,52] When one or both the pyridylmethyl arms in **1** are replaced by 6-methylpyridylmethyl arms to get **2** or **3**, the ν_1 band energy decreases, which is expected of the weaker coordination of sterically hindering 6-methylpyridyl nitrogen. Also, upon replacing the acyclic diamine in **5** by the cyclic diamine backbone as in **1**, the ν_1 band energy increases, which illustrates that the N4 ligands with diazapane backbone possess chelating ability higher than the analogous acyclic N4 ligand (Fig. 5a). Interestingly, when both the pyridylmethyl arms in **1** are replaced by imidazolylmethyl arms to get **4**, the ν_1 and ν_2 bands disappear and a peak around 446 nm is observed. This feature is assigned to $^1A_{1g} \rightarrow {}^1A_{2g}$ ligand field transition in Ni(II) with a square planar coordination geometry,[45,50] (Fig. 5b) and this confirms that N4 ligands with diazapane backbone possess higher ligand field strengths.

View Article Online
DOI: 10.1039/C7DT00576H

Functionalization of alkanes

The catalytic activity of **1-5** towards oxidation of cyclohexane and adamantane was investigated by using *m*-CPBA as oxidant in CH_2Cl_2:CH_3CN solvent mixture (3:1 v/v) at room temperature and the results are collected in Tables 4-6. When H_2O_2/*t*-BuOOH was used as oxidant, only trace amounts of oxidized products were detected (results are not shown here), revealing that the complexes are not effective as catalysts. In contrast, when *m*-CPBA was used as oxidant, **1**–**5** act as good catalysts; cyclohexane is oxidized efficiently with 340-601 total TON, with cyclohexanol (A) as the major product (TON, 290-527) and cyclohexanone (K; TON, 12-22) and ε-caprolactne (L) as the minor product (TON, 34-70), the alcohol-ketone selectivity (A/K, 5.6-7.2) being appreciable. Thus, only very small amounts of the oxidized products (cyclohexane, 8 TON; adamantane, 12 TON) were observed in the absence of complexes with *m*-CPBA as oxidant.[31, 53] The product ε-caprolactone is the over oxidized product of oxidation of cyclohexanone, effected by excess or unreacted *m*-CPBA. Also, the total TON for cyclohexane oxidation under air is lower than that under nitrogen atmosphere, revealing that any radical intermediate generated during catalytic cycle (cf. below) is quenched by dioxygen/moisture in air, leading to the decrease in yield. Also, the complexes catalyze the selective oxidation of adamantane to give up to 676 total TON with good to high regioselectivity between the tertiary (3°) and secondary (2°) carbons (3°/2° bond selectivity, 11.7).

The complex **1** catalyzes the oxidation of cyclohexane to give a total TON of 542 (TON: A, 460; K, 12; A/K, 5.6; L,70), which corresponds to 54% conversion of the oxidant to organic products. In order to illustrate the products formed and the trend in catalytic activity, we propose that *m*-CPBA binds to nickel(II) by replacing the labile acetonitrile molecules in $[Ni(L1)(CH_3CN)_2]^{2+}$ to give the intermediate adduct species $[Ni^{II}(L1)(OOCOC_6H_4Cl)]^+$. The latter undergoes O-O bond homolysis leading to the formation of putative $[(L1)Ni^{II}\text{-}O^{\bullet}]$/$[(L1)Ni^{III}\text{-}O]$ intermediate species and *m*-chlorobenzoic acid radical (Scheme 4). The formation of chlorobenzene (69–75% corresponding to total TON) supports this pathway.[30-32] We did not observe other products like *m*-chlorophenol or *m*-chlorobenzoic acid, which excludes the contribution of heterolytic O-O bond cleavage pathway. The high-spin (S = 3/2) radical intermediate $[(L1)Ni^{II}\text{-}O^{\bullet}]$ (**rad**$_{int}$) then abstracts the equatorial hydrogen atom of cyclohexane to form $[(L1)Ni^{II}(OH)]^+$ species and a cyclohexyl radical (Scheme 5).[31] Subsequently, the latter

View Article Online
DOI: 10.1039/C7DT00576H

reacts over through the C-O rebound step to form the cyclohexanol product. DFT calculations[31] on Ni(II) complexes of N5 ligands support the homolytic cleavage

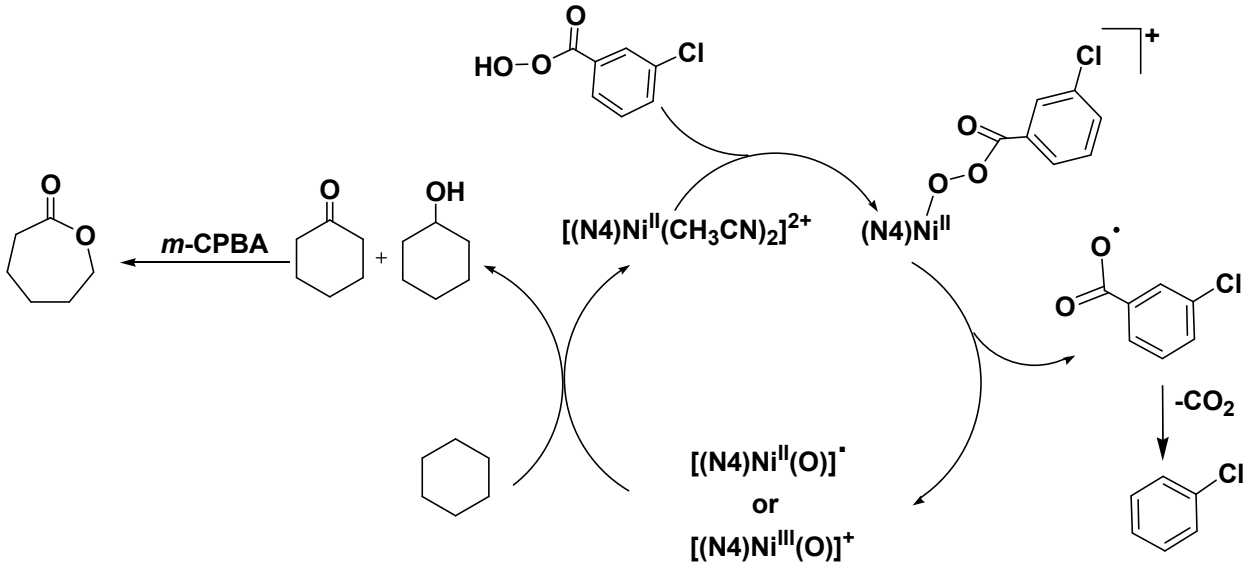

Scheme 4. Proposed mechanism of alkane hydroxylation

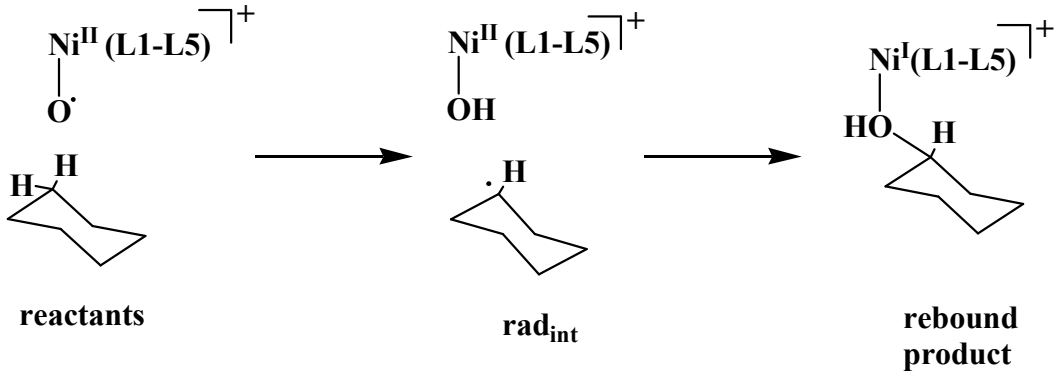

Scheme 5. Proposed mechanism for $[(L1\text{-}L5)Ni^{II}\text{-}O^{\bullet}]^{+}$ catalyzed cyclohexane oxidation/hydroxylation.

of O-O bond in $[Ni^{II}(N5)(OOCOC_6H_4Cl)]^{+}$ to give the high-spin (S = 3/2) intermediate species $[(N5)Ni^{II}\text{-}O^{\bullet}]/[(N5)Ni^{III}\text{-}O]$. We have previously invoked such an intermediate species to successfully illustrate the trends in catalytic activity of nickel(II) complexes of N4[30] and N5[31] ligands towards alkane hydroxylation. The adduct species $[Ni^{II}(L1)(OOCOC_6H_4Cl)]^{+}$ is suggested as five-coordinate with the bulky *m*-CPBA anion bound to Ni(II) in the axial position on the basis of the X-ray structures (cf. above) of $[Ni^{II}(L1)Cl]^{+}$ [45] and $[Ni^{II}(L4)Cl]^{+}$.[45] Thus, all

View Article Online
DOI: 10.1039/C7DT00576H

the present N4 ligands with diazapane backbone tend to form four-, five- and six-coordinate complexes, but make available only one axial site effectively for binding of oxidant. This is in contrast to $[Ni(L5)(CH_3CN)_2]^{2+}$ **5**, which makes available two cis coordination sites, leading to higher catalytic activity.

The time course of the TON for **1** in cyclohexane oxidation is shown in Fig. 6 and Table 4, which clearly indicates that the catalytic activity of the complex gradually proceeds even after 30 minutes. The catalytic activity increases from the total TON of 75 to 542 with the alcohol selectivity (A/K) also increasing from 1.1 to 5.7. When the number of equivalents of *m*-CPBA is increased with an aim to enhance the concentration of the intermediate and hence the reactivity, the amount of ε-caprolactone formed increases, confirming that ε-caprolactone results from secondary oxidation of cyclohexanone by the oxidant.

Effect of ligand donors

It is interesting that the catalytic activity of **1**-**5** towards cyclohexane oxidation varies as **5** > **1** > **2** > **3** > **4**. Upon moving from **1** to **2**, cyclohexane is catalytically oxidized with decrease in the total TON from 542 to 494 (TON: A, 422; K, 17; L, 55) and slight increase in alcohol selectivity (A/K, 5.9). When methyl groups are incorporated on both the pyridyl rings in **1** to get **3**, the total TON decreases further, from 542 to 456 (TON: A, 393; K, 15; L, 48; A/K 6.2) with slight increase in alcohol selectivity. The methyl group(s) introduced at 6-position of one (**2**) or both (**3**) the pyridyl rings sterically hinder(s) the coordination of pyridyl nitrogen and stabilizes the reactive nickel-oxo species and hence the lower catalytic activity of **2** and **3**. Also, the incorporation of methyl substituent(s) renders the binding of solvent molecules stronger (cf. above), making their substitution by the oxidant difficult. Upon replacing both the pyridylmethyl arms in **1** by two imidazolylmethyl arms to obtain **4**, the oxidation of cyclohexane takes place with substantial decrease in total TON from 542 to 340 (TON: A, 290; K, 16; L, 34) but with enhancement in selectivity (A/K, 7.2). The strongly σ-bonding [pK_a (BH^+): pyridine, 5.2; imidazole, 7.01], but weakly π-bonding imidazolyl nitrogen causes spin-pairing in **4**, which renders the formation of reactive high-spin (S = 3/2) intermediate [$(L4)Ni^{II}$-$O^{\bullet}$] species difficult, causing a decreased reactivity. It should be noted that only a very small amount of energy (+5.8 kcal/mol) is required to convert the low-spin catalyst to a reactive high-spin species. Interestingly, when the cyclic diamine moiety in **1** is substituted by ethylenediamine moiety to

View Article Online
DOI: 10.1039/C7DT00576H

obtain **5**, cyclohexane is catalytically oxidized with increase in TON from 542 to 601 (TON: A, 527; K, 22: L, 52) as well as alcohol selectivity (A/K, 7.1). The *cis*-β coordination geometry of **5** favors formation and stabilization of the reactive nickel-oxo intermediate. It is interesting that the presence of two cis-labile coordination sites is the key structural aspect for the improved catalysis of water oxidation by $[Ni(L5)(H_2O)_2]^{2+}$ with *cis*-α coordination geometry[48,54] We have observed that the *cis*-α complex $[Ni(iso\text{-}BPMEN)(CH_3CN)_2](BPh_4)_2$, where *iso*-BPMEN is *N*,*N*-dimethyl-*N',N'*-bis(pyrid-2-ylmethyl)ethane-1,2-diamine,[30] gives enhanced total TON of 622. Similar enhanced catalytic activity has been observed previously for nickel(II) complexes[25-27,30] with two labile *cis* positions.

Adamantane oxidation

Adamantane is efficiently oxidized by **1**- **5** to give 1-adamantanol and 2-adamantanol as the major products along with a small amount of 2-adamantanone as the minor product (Table 6). The trend in the catalytic activity is **5** > **1** > **2** > **3** > **4**, which is the same as that for cyclohexane oxidation; this suggests the involvement of the same high-valent nickel-oxo intermediate species in adamantane oxidation also. Complex **1** catalyzes the oxidation of adamantane to give a total TON of 589 with high 3°/2° bond selectivity (9.5). Upon moving from **1** to **2** the total TON decreases to 564 but with a slight increase in 3°/2° bond selectivity (10.2). Similarly, upon moving from **1** to **3**, the total TON decreases further to 525 with slight increase in 3º/2º bond selectivity (9.9), supporting the steric effect of methyl substituent on pyridyl ring (cf. above) in destabilizing the reactive intermediate species $[(L1)Ni^{II}\text{-}O^{\bullet}]$. Upon moving from **1** to **4** the oxidation of adamantane takes place with decrease in both the total TON (419) and 3°/2° bond selectivity (8.7). The replacement of both the pyridylmethyl arms in **1** by two imidazolylmethyl arms leads to spin-pairing in **4**, which renders formation of the reactive intermediate $[(L4)Ni^{II}\text{-}O^{\bullet}]$ species with high-spin (S = 3/2) configuration difficult, causing a decrease in reactivity. Interestingly, as observed for cyclohexane oxidation, the replacement of the cyclic diazapane backbone in **1** by ethylenediamine backbone to get **5**, both the total TON (676) and 3°/2° bond selectivity (11.7) increase. This supports the above finding that labile *cis* sites on nickel(II) facilitate ligand exchange with the oxidant, leading to good catalytic activity and selectivity.

View Article Online
DOI: 10.1039/C7DT00576H

Thus, a good π-back bonding pyridine donor facilitates the formation and stabilization of high-valent nickel-oxo species; however, incorporation of sterically demanding 6-methyl substituent adjacent to pyridyl nitrogen destabilizes it. Also, the ability of the N4 ligands with diazacyclo back bone have the potential to confer both high- and low-spin configurations on the Ni(II) catalysts, as dictated by pyridyl and imidazolyl nitrogens, and also steric hindrance to coordination would determine the catalytic activity towards alkane oxidation.

Conclusions

A few novel nickel(II) complexes of tetradentate N4 ligands with diazacyclo back bone have been isolated, their coordination geometries assessed and their potential to carry out alkane hydroxylation using *m*-CPBA as oxidant investigated. The Ni(II) complex of bis(pyridyl)-diaza ligand possesses a distorted octahedral coordination geometry whereas its bis(imidazole)-diaza analogue possesses a low-spin distorted square planar geometry. DFT studies throw light on the role of donor atom type, steric hindrance to coordination of pyridyl nitrogen, incorporation of diaazcyclo back bone and chelate ring sizes in conferring on Ni(II) novel coordination geometries - octahedral, high-spin square pyramidal and low-spin square planar. The present N4 ligands with diazacyclo back bone meridionally coordinate to Ni(II) but provide only one labile axial site for binding of the oxidant, and catalyze the oxidation of cyclohexane and adamantane with appreciably high TON and selectivity. In contrast, the corresponding linear N4 ligand with ethylenediamine back bone, which favor *cis*-α or *cis*-β octahedral configuration depending on solvent of coordination, provides two *cis* labile sites leading to higher catalytic activity. Thus, a robust Ni(II) catalyst for alkane oxidation may be designed by incorporating strongly π-back bonding heterocyclic nitrogen donors on a linear ethylenediamine-based tetradentate ligand.

Acknowledgments

This work is supported by the Science and Engineering Research Board (SERB) (Scheme No. EMR/2015/002222). Professor M. Palaniandavar is Indian National Science Academy (INSA) Honorary Scientist. We sincerely thank the Council of Scientific and Industrial Research (CSIR), New Delhi, for the Senior Research Fellowship to M.S and the Department of Science and Technology, SERB, for the award of Fast-track Young Scientist Fellowship to P.V. (Ref. No. CS-232/2012). We thank Department of Science and Technology (FIST program), New Delhi

View Article Online
DOI: 10.1039/C7DT00576H

for the use of the X-ray diffractometer at School of Chemistry. We thank Dr. K. Maheswari (deceased) for collecting the X-ray data for complex **1**. We thank Dr. Balachandran Unni Nair, Central Leather Research Institute, Chennai for providing the ESI-MS facility.

Supporting information

The crystal structures of **1** and **4** have been deposited at the Cambridge Crystallographic Data Centre and the deposition numbers allotted are CCDC 1400220 and CCDC 1400221. The data can be obtained free of charge via http://www.ccdc.cam.ac.uk/conts/retrieving.html, or from the Cambridge Crystallographic Data Centre, 12 Union Road, Cambridge CB2 1EZ, UK; fax: (+44) 1223-336-033; or e-mail: deposit@ccdc.cam.ac.uk.

References

1. (*a*) E. A. Lewis and W. B. Tolman, *Chem. Rev.,* 2004, **104**, 1047; (*b*) L. M. Mirica, X. Ottenwaelder and T. D. P. Stack, *Chem. Rev.,* 2004, **104**, 1013.

2. (*a*) J. B. Vincent, G. L. Olivier-Lilley and B. A. Averill, *Chem. Rev.,* 1990, **90**, 1447; (*b*) J. D. Lipscomb, *Annu. Rev. Microbiol.,*1994, **48**, 371.

3. (*a*) A. L. Feig and S. J. Lippard, *Chem. Rev.,* 1994, **94**, 759; (*b*) B. J. Waller and J. D. Lipscomb, *Chem. Rev.,*1996, **96**, 2625; (*c*) M. Baik, M. Newcomb, R. A. Friesner and S. J. Lippard, *Chem. Rev.,* 2003, **103**, 2385.

4. (*a*) M. Costas, M. P. Mehn, M. P. Jensen and L. Que, Jr., *Chem. Rev.,* 2004, **104**, 939; (*b*) E. Y. Tshuva and S. J. Lippard, *Chem. Rev.,* 2004, **104**, 987; (*c*) S. V. Kryatov, E. V. Rybak-Akimova and S. Schindler, *Chem. Rev.,* 2005, **105**, 2175.

5. (*a*) W. Nam, R. Ho and J. S. Valentine, *J. Am. Chem. Soc.,* 1991, **113**, 7052; (*b*) M. Kodera, H. Shimakoshi and K. Kano, *Chem.Commun.,*1996, 1737; (*c*) K. Chen and L. Que, Jr., *Chem. Commun.,* 1999, 1375.

6. (*a*) K. Chen and L. Que, Jr., *Angew. Chem., Int. Ed.,* 1999, **38**, 2227; (*b*) K. Chen and L. Que, Jr., *J. Am. Chem. Soc.,* 2001, **123**, 6327; (*c*) Y. Mekmouche, S. Ménage, C. Toia-Duboc, M. Fontecave, J.-B. Galey, C. Lebrun and J. Pécaut, *Angew. Chem., Int. Ed.,* 2001, **40**, 949; (*d*) G. Xue, R. D. Hont, E. Münck and L. Que, Jr., *Nature Chem.,* 2010, **2**, 400.

7. (*a*) M. Sankaralingam and M. Palaniandavar, *Polyhedron,* 2014, **67**, 171; (*b*) M. Balamurugan, E. Suresh and M. Palaniandavar, *Dalton Trans.,* 2016, **45**, 11422.

8. (*a*) M. Costas, K. Chen and L. Que, Jr., *Coord. Chem. Rev.,* 2000, **200**, 517; (*b*) D. H. R. Barton and D. Doller, *Acc. Chem. Res.,* 1992, **25**, 504; (*c*) A. E. Shilov and A. A.

View Article Online
DOI: 10.1039/C7DT00576H

Shteinman, *Acc. Chem. Res.* 1999, **32**, 763; (*d*) P. Stavropoulos, R. Çelenligil- Çetin and A. E. Tapper, *Acc. Chem. Res.,* 2001, **34**, 745; (*e*) T. Punniyamurthy, S. Velusamy and J. Iqbal, *Chem. Rev.,* 2005,**105**, 2329.

9. K. Nehru, S. J. Kim, I. Y. Kim, M. S. Seo, Y. Kim, S.-J. Kim, J. Kim and W. Nam, *Chem. Commun.,* 2007, 4623.

10. (*a*) M. Sankaralingam and M. Palaniandavar, *Dalton Trans.,* 2014, **43**, 538; (*b*) N. Saravanan, M. Sankaralingam and M. Palaniandavar, *RSC Adv.* 2014, **4**, 12000; (*c*) N. Saravanan and M. Palaniandavar, *Inorg. Chim. Acta.,* 2012, **385**, 100.

11. (*a*) N. W. Aboelella, S. V. Kryatov, B. F. Gherman, W. W. Brennessel, V. G. Young, Jr., R. Sarangi, E. V. Rybak-Akimova, K. O. Hodgson, B. Hedman, E. I. Solomon, C. J. Cramer and W. B. Tolman, *J. Am. Chem. Soc.,* 2004, **126**, 16896; (*b*) L. Que, Jr. and W. B. Tolman, *Angew. Chem., Int. Ed.,* 2002, **41**, 1114; (*c*) M. Suzuki, *Acc. Chem. Res.,* 2007, **40**, 609; (*d*) C. J. Cramer and W. B. Tolman, *Acc. Chem. Res.* 2007, **40**, 601; (*e*) S. Itoh and S. Fukuzumi, *Acc. Chem. Res.,* 2007, **40**, 592.

12. (*a*) J. R. Bryant, T. Matsuo and J. M. Mayer, *Inorg. Chem.,* 2004, **43**, 1587; (*b*) M. Yamaguchi, H. Kousaka, S. Izawa, Y. Ichii, T. Kumano, D. Masui and T. Yamagishi, *Inorg. Chem.,* 2006, **45**, 8342; (*c*) T. Kojima, K. Hayashi, S. Iizuka, F. Tani, Y. Naruta, M. Kawano, Y. Ohashi, Y. Hirai, K. Ohkubo, Y. Matsuda and S. Fukuzumi, *Chem.-Eur. J.,* 2007, **13**, 8212.

13. (*a*) S. Yiu, W. Man and T.-C Lau, *J. Am. Chem. Soc.,* 2008, **130**, 10821; (*b*) K. Jitsukawa, Y. Oka, S. Yamaguchi and H. Masuda, *Inorg. Chem.,* 2004, **43**, 8119; (*c*) M. Murali, R. Mayilmurugan and M. Palaniandavar, *Eur. J. Inorg. Chem.,* 2009, 3238.

14. J. F. Kinneary, J. S. Albert and C. J. Burrows, *J. Am. Chem. Soc.,* 1988, **110**, 6124.

15. (*a*) S. Hikichi, M. Yoshizawa, Y. Sasakura, M. Akita and Y. Moro-oka, *J. Am. Chem. Soc.,* 1998, **120**, 10567; (*b*) K. Shiren, S. Ogo, S. Fujinami, H. Hayashi, M. Suzuki, A. Uehara, Y. Watanabe and Y. Moro-oka, *J. Am. Chem. Soc.,* 2000, **122**, 254; (*c*) B. S. Mandimutsira, J. L. Yamarik, T. C. Brunold, W. Gu, S. P. Cramer and C. G. Riordan, *J. Am. Chem. Soc.,* 2001, **123**, 9194; (*d*) S. Hikichi, M. Yoshizawa, Y. Sasakura, H. Komatsuzaki, Y. Moro-oka and M. Akita, *Chem.-Eur. J.,* 2001, **7**, 5011.

16. (*a*) K. Fujita, R. Schenker, W. Gu, T. C. Brunold, S. P. Cramer and C. J. Riordan, *Inorg. Chem.,* 2004, **43**, 3324; (*b*) M. T. Kieber-Emmons, J. Annaraj, M. S. Seo, K. M. Van Heuvelen, T. Tosha, T. Kitagawa, T. C. Brunold, W. Nam and C. G. Riordan, *J. Am. Chem. Soc.,* 2006, **128**, 14230; (*c*) M. T. Kieber-Emmons and C. G. Riordan, *Acc. Chem. Res.* 2007, **40**, 618.

17. J. Cho, H. Furutachi, S. Fujinami and M. A. Suzuki, *Angew. Chem., Int. Ed.,* 2004, **43**, 3300.

View Article Online
DOI: 10.1039/C7DT00576H

18. S. Yao, E. Bill, C. Milsmann, K. Wieghardt and M. Driess, *Angew. Chem., Int. Ed.,* 2008, **47**, 7110.

19. A. Company, S. Yao, K. Ray and M. Driess, *Chem.-Eur. J.,* 2010, **16**, 9669.

20. S. Hikichi, C. Kobayashi, M. Yoshizawa and M. Akita, *Chem.-Asian. J.,* 2010, **5**, 2086.

21. T. Tano, Y. Doi, M. Inosako, A. Kunishita, M. Kubo, H. Ishimaru, T. Ogura, H. Sugimoto and S. Itoh, *Bull. Chem. Soc. Jpn.,* 2010, **83**, 530.

22. J. Cho, R. Sarangi, J. Annaraj, S. Y. Kim, M. Kubo, T. Ogura, E. I. Solomon and W. Nam, *Nature Chem.,* 2009, **1**, 568.

23. R. Latifi, L. Tahsini, D. Kumar, G. N. Sastry, W. Nam and S. P. de Visser, S. P. *Chem. Commun.,* 2011, **47**, 10674.

24. J. Cho, H. Y. Kang, L. V. Liu, R. Sarangi, E. I. Solomon and W. Nam, *Chem. Sci.,* 2013, **4**, 1502.

25. T. Nagataki, Y. Tachi and S. Itoh, *Chem. Commun.,* 2006, 4016.

26. T. Nagataki, K. Ishii, Y. Tachi and S. Itoh, *Dalton Trans.,* 2007, 1120.

27. (*a*) T. Nagataki and S. Itoh, *Chemistry Letters*, 2007, **36(6)**, 748; (*b*) Y. Morimoto, S. Bunno, N. Fujieda, H. Sugimoto and S. Itoh, *J. Am. Chem. Soc.,* 2015, **137**, 5867.

28. S. Hikichi, H. Okuda, Y. Ohzu and M. Akita, *Angew. Chem., Int. Ed.,* 2009, **48**, 188.

29. (*a*) J. Nakazawa, S. Terada, M. Yamada and S. Hikichi, *J. Am. Chem. Soc.,* 2013, **135**, 6010. (*b*) S. Hikichi, K. Hanaue, T. Fujimura, H. Okuda, J. Nakazawa, Y. Ohzu, C. Kobayashi and M. Akita, *Dalton Trans.,* 2013, **42**, 3346.

30. M. Balamurugan, R. Mayilmurugan, E. Suresh and M. Palaniandavar, *Dalton Trans.,* 2011, **40**, 9413.

31. M. Sankaralingam, M. Balamurugan, P. Vadivelu, C. H. Suresh and M. Palaniandavar, *Chem. Eur. J.,* 2014, **20**, 11346.

32. M. Sankaralingam, P. Vadivelu, E. Suresh and M. Palaniandavar, *Inorg. Chim. Acta.,* 2013, **407**, 98.

33. F. F. Pfaff, F. Heims, S. Kundu, S. Mebs and K. Ray, *Chem. Commun.,* 2012, **48**, 3730.

34. (*a*) T. Corona, F. F. Pfaff, F. Acuña-Parés, A. Draksharapu, C. J. Whiteoak, V. Martin-Diaconescu, J. Lloret-Fillol, W. R. Browne, K. Ray and A. Company, *Chem.-Eur. J.,* 2015, **21**, 15029; (*b*) T. Corona, A. Draksharapu, S. K. Padamati, I. Gamba, V. Martin-Diaconescu, F. Acuña-Parés, W. R. Browne and A. Company, *J. Am. Chem. Soc.,* 2016, **138**, 12987.

View Article Online
DOI: 10.1039/C7DT00576H

35. (*a*) P. Pirovano, E. R. Farquhar, M. Swart, A. J. Fitzpatrick, G. G. Morgan and A. R. McDonald, *Chem.-Eur. J.,* 2015, **21**, 3785; (*b*) P. Pirovano, E. R. Farquhar, M. Swart and A. R. McDonald, *J. Am. Chem. Soc.* 2016, **138**, 14362.

36. (*a*) K. H. Bok, Myoung, M. Lee, G. R. You, H. M. Ahn, K. Y. Ryu, S.-J. Kim, Y. Kim and C. Kim, *Chem.-Eur. J.,* 10.1002/chem.201605157; (*b*) A. R. Jeong, J. W. Shin, J. H. Jeong, K. H. Bok, C. Kim, D. Jeong, J. Cho, S. Hayami, K. S. Min, *Chem.-Eur. J.,* 10.1002/chem.201604498.

37. R. Mayilmurugan, H. S. Evans and M. Palaniandavar, *Inorg. Chem.* 2008, **47**, 6645.

38. P. Mialane, L. Tehertanov, F. Banse, J. Sainton and J. Girerd, *Inorg. Chem.,* 2000, **39**, 2440.

39. Gaussian 09, Revision A.1, M. J. Frisch, G. W. Trucks, H. B. Schlegel, G. E. Scuseria, M. A. Robb, J. R. Cheeseman, G. Scalmani, V. Barone, B. Mennucci, G. A. Petersson, H. Nakatsuji, M. Caricato, X. Li, H. P. Hratchian, A. F. Izmaylov, J. Bloino, G. Zheng, J. L. Sonnenberg, M. Hada, M. Ehara, K. Toyota, R. Fukuda, J. Hasegawa, M. Ishida, T. Nakajima, Y. Honda, O. Kitao, H. Nakai, T. Vreven, J. A. Montgomery, Jr., J. E. Peralta, F. Ogliaro, M. Bearpark, J. J. Heyd, E. Brothers, K. N. Kudin, V. N. Staroverov, R. Kobayashi, J. Normand, K. Raghavachari, A. Rendell, J. C. Burant, S. S. Iyengar, J. Tomasi, M. Cossi, N. Rega, J. M. Millam, M. Klene, J. E. Knox, J. B. Cross, V. Bakken, C. Adamo, J. Jaramillo, R. Gomperts, R. E. Stratmann, O. Yazyev, A. J. Austin, R. Cammi, C. Pomelli, J. W. Ochterski, R. L. Martin, K. Morokuma, V. G. Zakrzewski, G. A. Voth, P. Salvador, J. J. Dannenberg, S. Dapprich, A. D. Daniels, Ö. Farkas, J. B. Foresman, J. V. Ortiz, J. Cioslowski and D. J. Fox, Gaussian, Inc., Wallingford CT, 2009.

40. D. Andrae, U. Häusserman, M. Dolg, H. Stoll and H. Preuss, *Theor. Chim. Acta.*, 1990, **77**,123.

41. (*a*) W. J. Hehre, R. Ditchfield and J. A. Pople, *J. Chem. Phys.,* 1972, **56**, 2257; (*b*) P. C. Hariharan and J. A. Pople, *Theor. Chim. Acta.,* 1973, **28**, 213.

42. *CrysAlisPro*, Version 1.171.33.66; Oxford Diffraction Ltd.: Abingdon, U.K., 2010.

43. G. M. Sheldrick, *SHELXL* Version 2016/6.

44. *SADABS,* Empirical Absorption Correction Program; University of Göttingen: Göttingen, Germany, (1997).

45. Y.-M. Guo, M. Du and X.-H. Bu, *Inorg. Chim. Acta.,* 2005, **358**, 1887.

46. R. A. Geiger, S. Chattopadhyay, V. W. Day and T. A. Jackson, *J. Am. Chem. Soc.,* 2010, **132**, 2821.

47. D. C. Fox, A. T. Fiedler, H. L. Halfen, T. C. Brunold, and J. A. Halfen, *J. Am. Chem. Soc.,* 2004, **126**, 7627.

View Article Online
DOI: 10.1039/C7DT00576H

48. (*a*) M. S. Kryatova, O. V. Makhlynets, A. Y. Nazarenko and E. V. Rybak-Akimova, *Inorg. Chim. Acta*., 2012, **387**, 74; (*b*) G.-Y. Luo, H.-H. Huang, J.-W. Wang and T.-B. Lu, *ChemSusChem,* 2016, **9**, 485.

49. C. Hureau, G. Blondin, M.-F. Charlot, C. Philouze, M. Nierlich, M. Césario and E. Anxolabéhère-Mallart, *Inorg. Chem.,* 2005, **44**, 3669.

50. R. M. Jenkins, M. L. Singleton, E. Almaraz, J. H. Reibenspies and M. Y. Darensbourg, *Inorg. Chem.,* 2009, **48**, 7280.

51. (*a*) M. Velusamy, M. Palaniandavar and K. R. Justin Thomas, *Polyhedron,* 1998, **17**, 2179. (*b*) A. B. P. Lever, Inorganic Electronic Spectroscopy, Elsevier (Second ed.) Amsterdam, (1986).

52. T. R. Holman, M. P. Hendrich and L. Que, Jr., *Inorg. Chem.,* 1992, **31**, 937.

53. A. Bravo, H.-R. Bjorsvik, F. Fontana, F. Minisci and A. Serri, *J. Org. Chem.,* 1996, **61**, 9409.

54. J. L. Fillol, Z. Codolà, I. Garcia-Bosch, L. Gómez, J. J. Pla and M. Costas, *Nat. Chem.,* 2011, **3**, 807.

View Article Online
DOI: 10.1039/C7DT00576H

Table 1. Crystallographic data for complexes **1** and **4**

	1	**4**
Empirical formula	$C_{69}H_{68}B_2N_6Ni$	$C_{63}H_{64}B_2N_6Ni$
Formula weight /g mol^{-1}	1061.63	985.53
Crystal habit, color	Purple	Yellow
Crystal system	Monoclinic	Monoclinic
Crystal size	0.12 x 0.09 x 0.06 mm	0.23 x 0.10 x 0.09 mm
Space group	$P2_1/c$	$P2_1/n$
a, Å	11.6625(4)	16.5550(7)
b, Å	13.6676(4)	12.0464(4)
c, Å	35.5420(11)	27.2008(13)
α, deg	90	90
β, deg	95.268 (3)	106.496(5)
γ, deg	90	90
V/Å^3	5641.4(3)	5201.3(4)
Z	4	21
ρ_{calcd}/ g cm^{-3}	1.250	1.259
F(000)	2248	2088
Temperature (K)	150	293(2)
No. of Reflections collected	30859	65074
No. of unique reflections	13214 (R(int) = 0.0757)	14036 (R(int) = 0.1017)
Radiation(MoKα)/ Å	0.7107	0.7107
Goodness-of-fit on F^2	0.941	0.790
Number of refined Parameters	706	650
*R*1/ w *R*2[$I > 2\sigma(I)$][a]	$R_1 = 0.0669$, $wR_2 = 0.0735$	$R_1 = 0.0698$, $wR_2 = 0.1920$
*R*1/ w *R*2 (all data)	$R_1 = 0.1458$, $wR_2 = 0.0921$	$R_1 = 0.1483$, $wR_2 = 0.2689$

[a] $R1 = [\Sigma(||F_o|-|F_c||)/\Sigma|F_o|]$; $wR2 = \{[\Sigma(w(F_o^2-F_c^2)^2)/\Sigma(wF_o^4)]^{1/2}\}$

View Article Online
DOI: 10.1039/C7DT00576H

Table 2. Selected bond lengths [Å] and bond angles [°] for **1** and **4**

1		**4**	
Bond lengths/Å			
Ni(1)-N(2)	2.065(2)	Ni(1)-N(1)	1.869(3)
Ni(1)-N(3)	2.075(3)	Ni(1)-N(2)	1.915(3)
Ni(1)-N(5)	2.077(2)	Ni(1)-N(3)	1.909(3)
Ni(1)-N(6)	2.076(3)	Ni(1)-N(4)	1.892(3)
Ni(1)-N(8)	2.184(3)		
Ni(1)-N(10)	2.097(3)		
Bond angles/ °			
N(2)-Ni(1)- N(3)	82.68(10)	N(1)-Ni(1)- N(2)	87.45(14)
N(2)-Ni(1)- N(5)	159.94(11)	N(1)-Ni(1)- N(3)	170.27(14)
N(2)-Ni(1)- N(6)	117.22(10)	N(1)-Ni(1)- N(4)	103.25(16)
N(2)-Ni(1)- N(8)	86.86(10)	N(2)-Ni(1)- N(3)	82.83(14)
N(2)-Ni(1)- N(10)	85.55(11)	N(2)-Ni(1)- N(4)	167.46(15)
N(3)-Ni(1)- N(5)	77.63(10)	N(3)-Ni(1)- N(4)	86.41(16)
N(3)-Ni(1)- N(6)	159.69(10)		
N(3)-Ni(1)- N(8)	98.70(11)		
N(3)-Ni(1)- N(10)	93.24(11)		
N(5)-Ni(1)- N(6)	82.72(10)		
N(5)-Ni(1)- N(8)	99.79(10)		
N(5)-Ni(1)- N(10)	91.72(10)		
N(6)-Ni(1)- N(8)	79.51(10)		
N(6)-Ni(1)- N(10)	92.43(11)		
N(8)-Ni(1)- N(10)	164.92(10)		

View Article Online
DOI: 10.1039/C7DT00576H

Table 3. UV-visible spectral data of nickel(II) complexes[a] **1-5** in CH_2Cl_2:CH_3CN solvent mixture (3:1 v/v) at 25.0 °C

Complex	λ_{max}, nm (ε, M^{-1} cm^{-1})
1	472 (48),785 (35), 842 (36)
2	382 (103), 496 (sh), 600 (30),798 (27), 852 (29), 924 (34)
3	382 (125), 487 (24), 588 (37),763 (32), 893 (19)
4	243 (1820), 280 (145), 446 (130)
5	358 (sh), 565 (18), 773 (6), 924 (10)

[a]Concentration of nickel(II) complexes, 1.0×10^{-2} M

View Article Online
DOI: 10.1039/C7DT00576H

Table 4. Products of oxidation of cyclohexane catalyzed[a] by **1** with time

Time (min.)	Cyclohexane (TON)			Total TON[c]	A/K[d]	Yield[e] (%)
	-ol[b]	-one[b]	ε-caprolactone			
30	55	8	12	75(3)	1.1	7.5
60	176	17	25	218(3)	4.2	21.8
120	358	18	45	421(2)	5.7	42.1
240	424	14	63	501(2)	5.5	50.1
720	460	12	70	542(1)	5.6	54.2

[a]Reaction conditions: Catalyst (0.35×10^{-6} mol dm^{-3}), Substrate (2.45 mol dm^{-3}), Oxidant (0.35 mol dm^{-3}) in CH_2Cl_2: CH_3CN solvent mixture (3:1 v/v); [b]-ol = cyclohexanol and -one = cyclohexanone; [c]Total TON = no. of mmol of product/no. of mmol of catalyst; [d]A/K = TON of -ol/ (TON of -one + TON of ε-caprolactone); [e]Yield based on the oxidant.

Table 5. Products of oxidation of cyclohexane catalyzed[a] by Ni(II) complexes

Complex	Cyclohexane (TON)			Total TON[c]	Chloro-benzene	A/K[d]	Yield[e] (%)
	-ol[b]	-one[b]	ε-caprolactone				
Blank[f]	6.0	1.0	1.0	8.0	-	3.0	0.8
1	460	12	70	542(2)	376	5.6	54.2
2	422	17	55	494(3)	352	5.9	49.4
3	393	15	48	456(2)	332	6.2	45.6
4	290	16	34	340(3)	240	7.2	34.0
5	527	22	52	601(1)	453	7.1	60.1

[a]Reaction conditions: Catalyst (0.35×10^{-6} mol dm^{-3}), Substrate (2.45 mol dm^{-3}), Oxidant (0.35 mol dm^{-3}) in CH_2Cl_2: CH_3CN solvent mixture (3:1 v/v); [b]-ol = cyclohexanol and -one = cyclohexanone; [c]Total TON = no. of mmol of product/no. of mmol of catalyst; [d]A/K = TON of -ol/ (TON of -one + TON of ε-caprolactone); [e]Yield based on the oxidant. [f]Blank = Substrate (2.45 mol dm^{-3}), Oxidant (0.35 mol dm^{-3}) in CH_2Cl_2:CH_3CN solvent mixture (3:1 v/v).

View Article Online
DOI: 10.1039/C7DT00576H

Table 6. Products of oxidation of adamantane catalyzed[a] by Ni(II) complexes

Complex	Adamantane (TON)			Total TON[c]	Selectivity[d]	Yield[e]
	1-adol[b]	2-adol[b]	2-adone[b]		3°/2°	(%)
Blank[f]	8.0	2.4	1.6	12.0	6.0	1.2
1	448	131	10	589(2)	9.5	58.9
2	436	112	16	564(2)	10.2	56.4
3	403	110	12	525(2)	9.9	52.5
4	312	95	12	419(3)	8.7	41.9
5	538	120	18	676(2)	11.7	67.6

[a]Reaction conditions: Catalyst (0.2×10^{-6} mol dm^{-3}), Substrate (0.4 mol dm^{-3}), Oxidant (0.2 mol dm^{-3}) in CH_2Cl_2: CH_3CN solvent mixture (3:1 v/v); [b]1-adol = 1-adamantanol, 2-adol = 2-adamantanol and 2-adone = 2-adamantanone; [c]TON = no. of mmol of product/no. of mmol of catalyst; [d]3°/2° = (TON of 1-adol×3)/(TON of 2-adol+ TON of 2-adone); [e]Yield based on the oxidant. [f]Blank = Substrate (0.4 mol dm^{-3}), Oxidant (0.2 mol dm^{-3}) in CH_2Cl_2:CH_3CN solvent mixture (3:1 v/v).

View Article Online
DOI: 10.1039/C7DT00576H

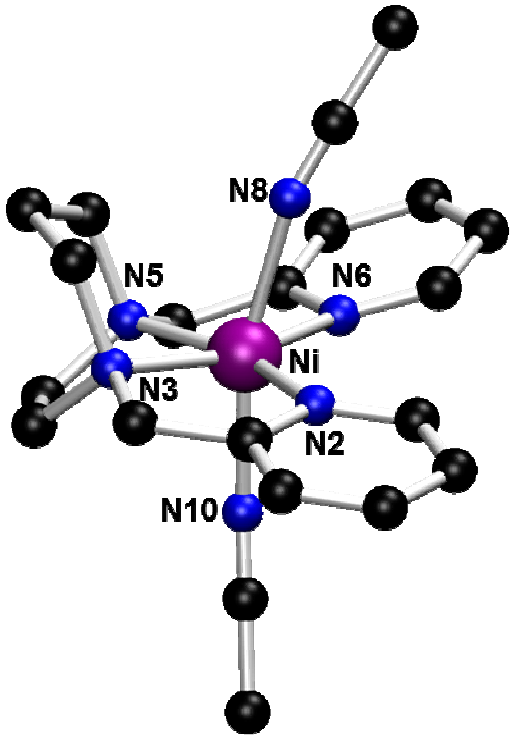

Fig. 1 ORTEP diagram of $[Ni(L1)(CH_3CN)_2]^{2+}$ complex **1** showing 45% probability thermal ellipsoids and the labeling scheme for selected atoms. All hydrogen atoms are omitted for clarity.

View Article Online
DOI: 10.1039/C7DT00576H

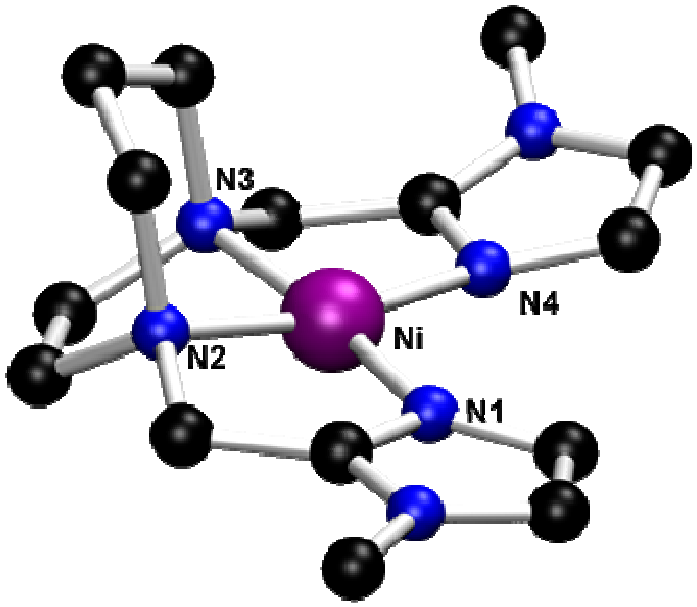

Fig. 2 ORTEP diagram of $[Ni(L4)]^{2+}$ complex **4** showing 50% probability thermal ellipsoids and the labeling scheme for selected atoms. All hydrogen atoms are omitted for clarity.

View Article Online
DOI: 10.1039/C7DT00576H

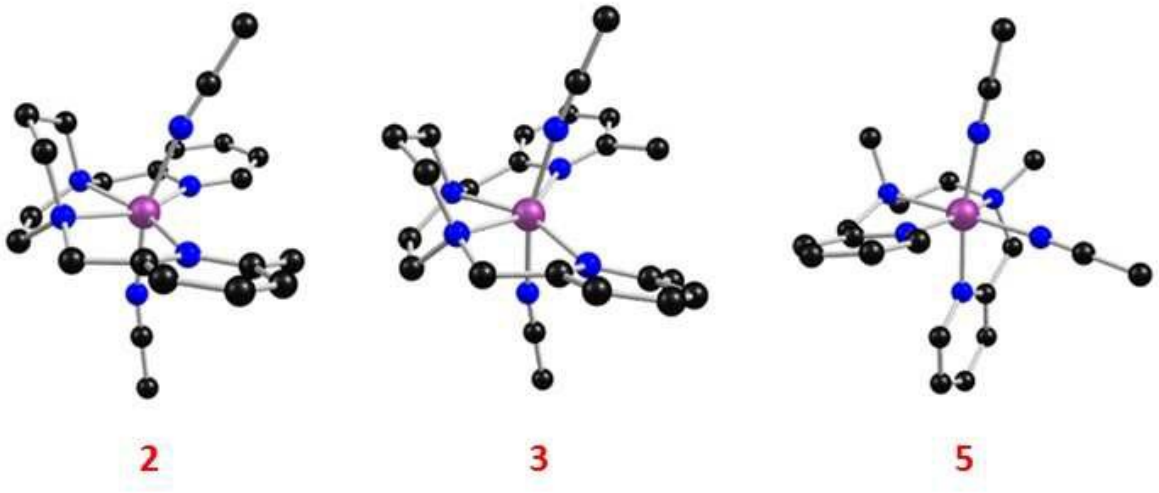

Fig. 3 DFT optimized coordination geometries of $[Ni(L2)(CH_3CN)_2]^{2+}$ **2**, $[Ni(L3)(CH_3CN)_2]^{2+}$ **3** and $[Ni(L5)(CH_3CN)_2]^{2+}$ **5**.

View Article Online
DOI: 10.1039/C7DT00576H

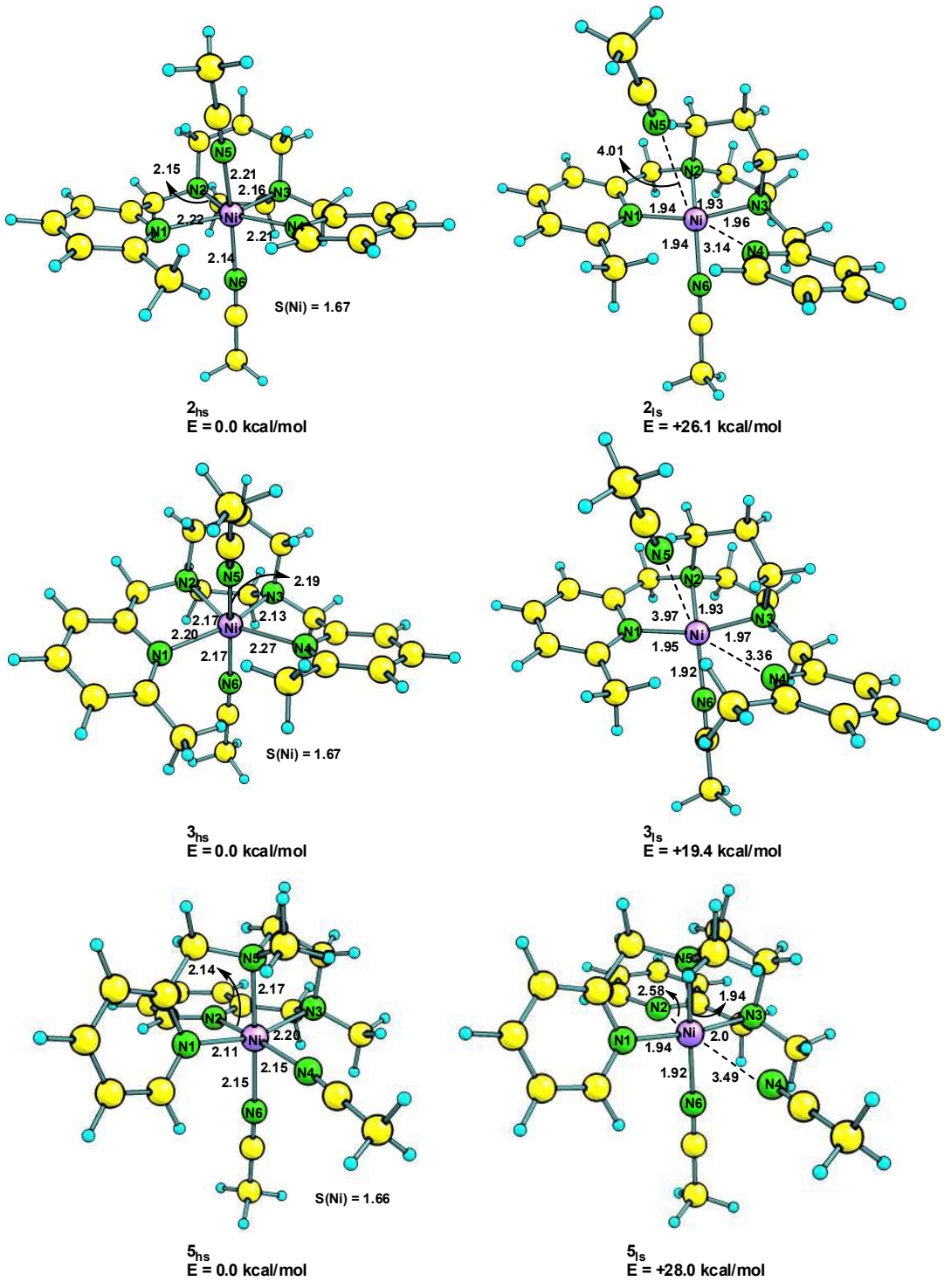

Fig. 4 DFT optimized geometries of **2**, **3** and **5** in the high- and low-spin state configurations.

View Article Online
DOI: 10.1039/C7DT00576H

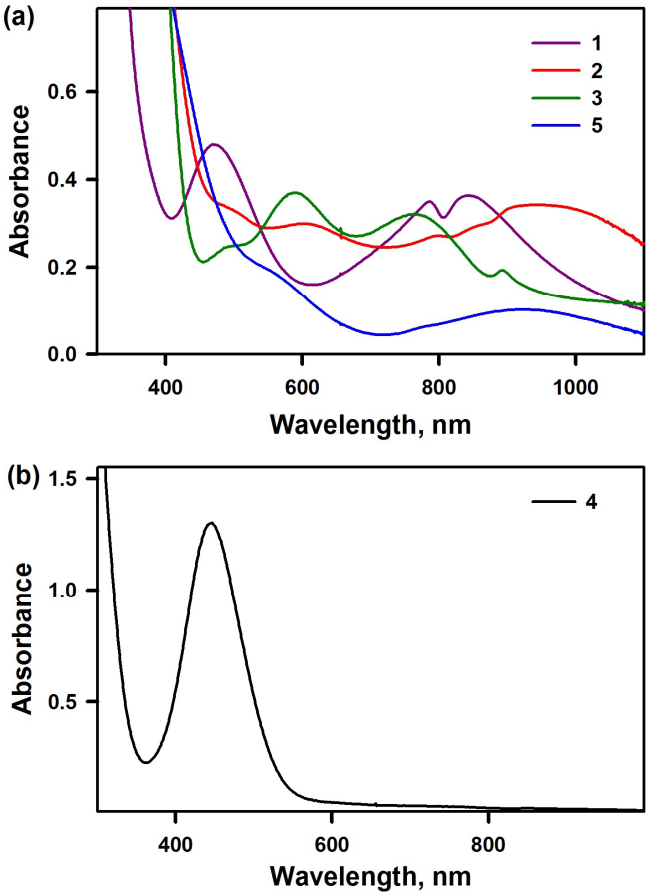

Fig. 5 Electronic absorption spectra of complexes (a) 1.0×10^{-2} M solutions of **1-3** and **5** in CH_2Cl_2:CH_3CN solvent mixture (3:1 v/v) at 25.0 ^{o}C. (b) 1.0×10^{-2} M solution of **4** in CH_2Cl_2:CH_3CN solvent mixture (3:1 v/v) at 25.0 ^{o}C.

View Article Online
DOI: 10.1039/C7DT00576H

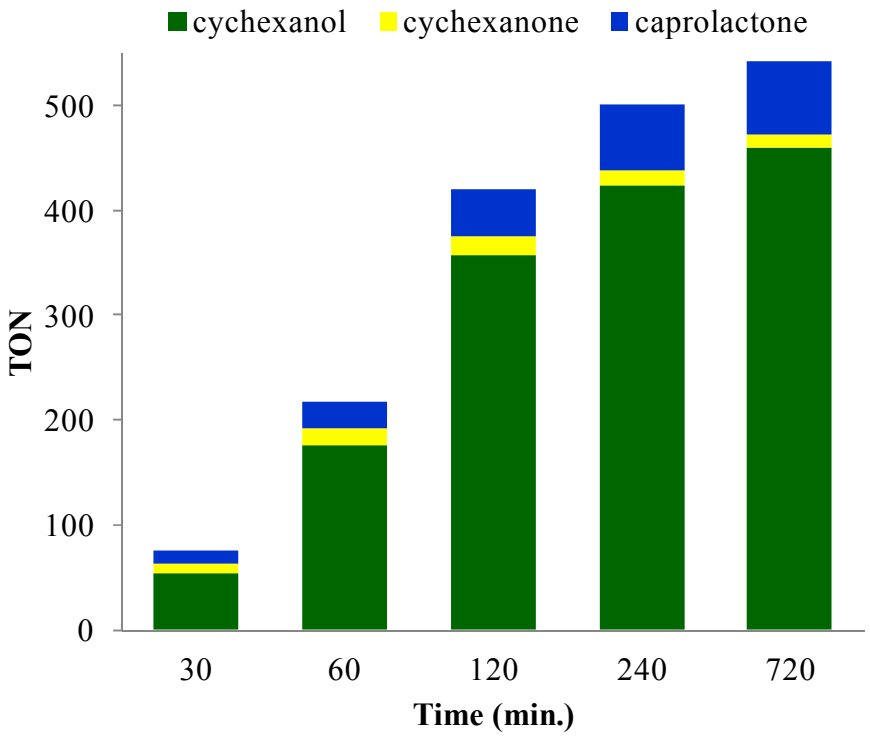

Fig. 6 Bar chart representation of conversion of cyclohexane catalyzed by **1** with time in CH_2Cl_2: CH_3CN solvent mixture (3:1 v/v) at room temperature.

View Article Online
DOI: 10.1039/C7DT00576H

Graphical Abstract

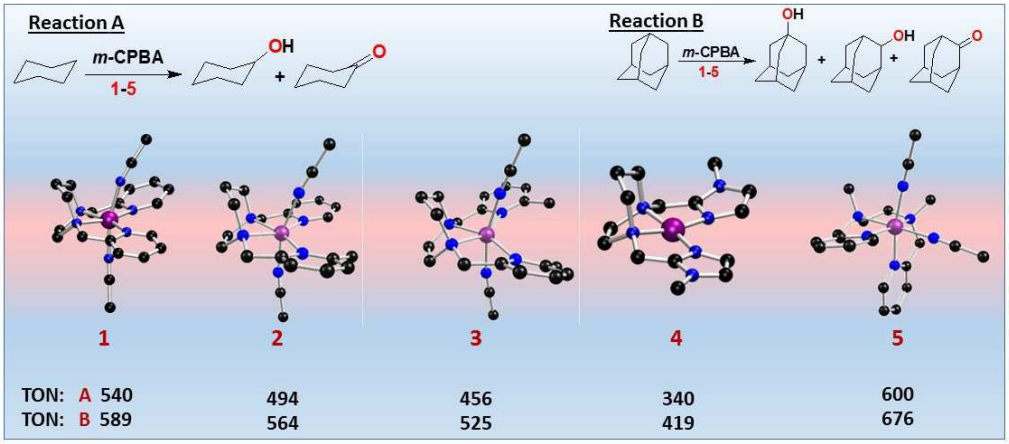

The stereoelectronic factors of linear N4 ligands with diazacyclo backbone and solvent of coordination dictate the Ni(II) spin state (**4**, low-spin; **1**-**3**,**5**, high-spin) and catalytic activity of the complexes towards hydroxylation of cyclohexane and adamantane using *m*-CPBA as oxidant.